

Frascati Physics Series Vol. LXIII (2016), pp. 00-00
5th YOUNG RESEARCHERS WORKSHOP: “Physics Challenges in the LHC Era”
Frascati, May 9 and 12, 2016

BFKL phenomenology: resummation of high-energy logs in semi-hard processes at LHC

Francesco Giovanni Celiberto

*Dipartimento di Fisica, Università della Calabria,
Istituto Nazionale di Fisica Nucleare, Gruppo Collegato di Cosenza
Arcavacata di Rende, 87036 Cosenza, Italy*

Abstract

A study of differential cross sections and azimuthal observables for semi-hard processes at LHC energies, including BFKL resummation effects, is presented. Particular attention has been paid to the behaviour of the azimuthal correlation momenta, when a couple of forward/backward jets or identified hadrons is produced in the final state with a large rapidity separation. Three- and four-jet production has been also considered, the main focus lying on the definition of new, generalized azimuthal observables, whose dependence on the transverse momenta and the rapidities of the central jet(s) can be considered as a distinct signal of the onset of BFKL dynamics.

1 Introduction

The large amount of data already recorded and to be produced in the near future at the Large Hadron Collider (LHC) offers a peerless opportunity to

probe perturbative QCD at high energies. Multi-Regge kinematics (MRK), which prescribes the production of strongly rapidity-ordered objects in the final state, is the key point for the study of semi-hard processes in the high-energy limit. In this kinematical regime, the Balitsky-Fadin-Kuraev-Lipatov (BFKL) approach, at leading (LL) [1–6] and next-to-leading (NLL) [7, 8] accuracy, represents perhaps the most powerful tool to perform the resummation of large logarithms in the colliding energy to all orders of the perturbative expansion. So far, Mueller–Navelet jet production [9] has been the most studied reaction. Interesting observables associated to this process are the azimuthal correlation momenta, which, however, are strongly affected by collinear contaminations. Therefore, new observables, independent from these contaminations, were proposed in [10, 11] and calculated at NLL in [12–21], showing a very good agreement with experimental data at the LHC. Unfortunately, Mueller–Navelet configurations are still too inclusive to perform MRK precision studies. With the aim to further and deeply probe the BFKL dynamics, we propose to investigate two different kinds of processes. The first one is the detection of two charged light hadrons: π^\pm , K^\pm , p , \bar{p} having high transverse momenta and separated by a large interval of rapidity, together with an undetected hadronic system X [22, 23]. On one side, hadrons can be detected at the LHC at much smaller values of the transverse momentum than jets, allowing us to explore a kinematic range outside the reach of the Mueller–Navelet channel. On the other side, this process makes it possible to constrain not only the parton densities (PDFs) for the initial proton, but also the parton fragmentation functions (FFs) describing the detected hadron in the final state. The second kind of processes is the multi-jet production [24–27], which allows to define new, generalized and suitable BFKL observables by considering extra jets well separated in rapidity in the final state and by studying the dependence on their transverse momenta and azimuthal angles.

2 Di-hadron production

We consider the production, in high-energy proton-proton collisions, of a pair of identified hadrons with large transverse momenta, $\vec{k}_1^2 \sim \vec{k}_2^2 \gg \Lambda_{\text{QCD}}^2$ and large separation in rapidity. The differential cross section of the process reads

$$\frac{d\sigma^{\text{di-hadron}}}{dy_1 dy_2 d|\vec{k}_1| d|\vec{k}_2| d\phi_1 d\phi_2} = \frac{1}{(2\pi)^2} \left[C_0 + \sum_{n=1}^{\infty} 2 \cos(n\phi) C_n \right], \quad (1)$$

where $\phi = \phi_1 - \phi_2 - \pi$, with $\phi_{1,2}$ the two hadrons’ azimuthal angles, while $y_{1,2}$ and $\vec{k}_{1,2}$ are their rapidities and transverse momenta, respectively. In order to match the kinematic cuts used by the CMS collaboration, we consider the

integrated azimuthal coefficients given by

$$C_n = \int_{y_{1,\min}}^{y_{1,\max}} dy_1 \int_{y_{2,\min}}^{y_{2,\max}} dy_2 \int_{k_{1,\min}}^{\infty} dk_1 \int_{k_{2,\min}}^{\infty} dk_2 \delta(y_1 - y_2 - Y) C_n \quad (2)$$

and their ratios $R_{nm} \equiv C_n/C_m$. For the integrations over rapidities and transverse momenta we use the limits, $y_{1,\min} = -y_{2,\max} = -2.4$, $y_{1,\max} = -y_{2,\min} = 2.4$, $k_{1,\min} = k_{2,\min} = 5$ GeV, which are realistic values for the identified hadron detection at LHC. In Fig. 1 the dependence on the rapidity separation between the detected hadrons, $Y = y_1 - y_2$, of the ϕ -averaged cross section C_0 and of the ratios R_{10} and R_{20} at the center-of-mass energy $\sqrt{s} = 13$ TeV is shown.

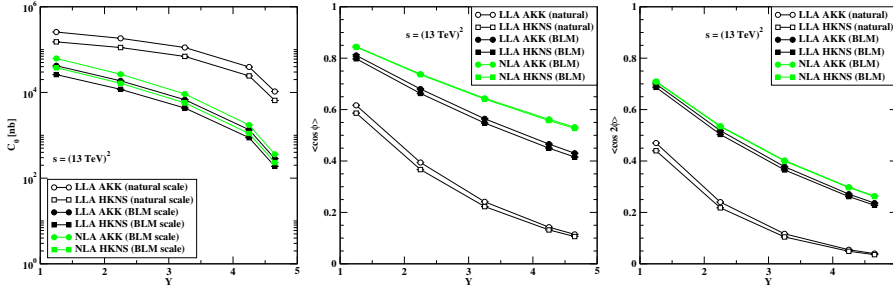


Figure 1: Y dependence of cross section, $\langle \cos \phi \rangle$ and $\langle \cos 2\phi \rangle$ for di-hadron production at $\sqrt{s} = 13$ TeV. See Ref. [23] for the FF parametrizations used and for the definition of “natural” and “BLM” scales.

3 Multi-jet production

The process under investigation is the hadroproduction of n jets in the final state, well separated in rapidity so that $y_i > y_{i+1}$ according to MRK, and with their transverse momenta $\{k_i\}$ lying above the experimental resolution scale, together with an undetected soft-gluon radiation emission. Pursuing the goal to generalize the azimuthal ratios R_{nm} defined for Mueller–Navelet jet and di-hadron production, we define new, generalized azimuthal correlation momenta by projecting the differential cross section $d\sigma^{n\text{-jet}}$ on all angles, so having

$$\mathcal{C}_{M_1 \dots M_{n-1}} = \left\langle \prod_{i=1}^{n-1} \cos(M_i \phi_{i,i+1}) \right\rangle = \int_0^{2\pi} d\theta_1 \dots \int_0^{2\pi} d\theta_n \prod_{i=1}^{n-1} \cos(M_i \phi_{i,i+1}) d\sigma^{n\text{-jet}} \quad (3)$$

where $\phi_{i,i+1} = \theta_i - \theta_{i+1} - \pi$, with θ_i being the azimuthal angle of the jet i . Firstly, we introduce realistic LHC kinematical cuts by integrating $\mathcal{C}_{M_1 \dots M_{n-1}}$

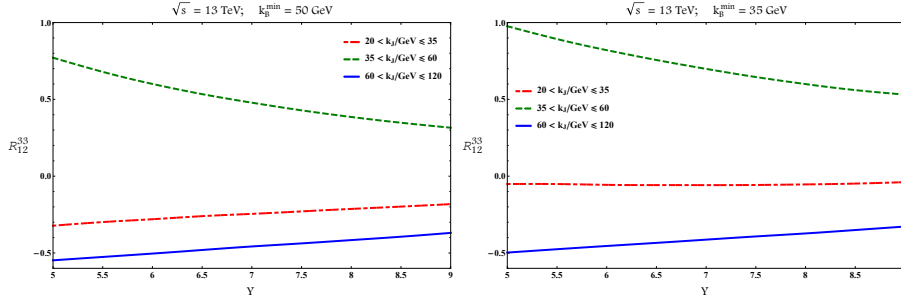


Figure 2: Y dependence of R_{12}^{33} for $\sqrt{s} = 13$ TeV and $k_{B,\min} = 50$ GeV (left column) and $k_{B,\min} = 35$ GeV (right column). $k_{A,\min}$ is fixed to 35 GeV, while the central jet has rapidity $y_J = (y_A + y_B)/2$.

over rapidities and momenta of the tagged jets

$$C_{M_1 \dots M_{n-1}} = \int_{y_{1,\min}}^{y_{1,\max}} dy_1 \dots \int_{y_{n,\min}}^{y_{n,\max}} dy_n \int_{k_{1,\min}}^{\infty} dk_1 \dots \int_{k_{n,\min}}^{\infty} dk_n \delta(y_1 - y_n - Y) \mathcal{C}_n \quad (4)$$

and by keeping fixed the rapidity difference $Y = y_1 - y_n$ between the most forward and the most backward jet, which corresponds to the maximum rapidity interval in the final state. Secondly, we remove the zeroth conformal spin contribution responsible for any collinear contamination and we minimise possible higher-order effects by studying the ratios $R_{N_1 \dots N_{n-1}}^{M_1 \dots M_{n-1}} \equiv C_{M_1 \dots M_{n-1}} / C_{N_1 \dots N_{n-1}}$ where $\{M_i\}$ and $\{N_i\}$ are positive integers. In Fig. 2 we show the dependence on Y of the coefficient R_{12}^{33} , characteristic of the 3-jet production process, for $\sqrt{s} = 13$ TeV, for two different kinematical cuts on the transverse momenta $k_{A,B}$ of the external jets and for three different ranges of the central jet transverse momentum k_J . In Fig. 3 we show the dependence on Y of the coefficient R_{112}^{221} , characteristic of the 4-jet production process, for $\sqrt{s} = 7$ and 13 TeV, for asymmetrical cuts on the transverse momenta $k_{A,B}$ of the external jets and for two different configurations of the central jet transverse momenta $k_{1,2}$. A comparison with predictions for these observables from fixed order analyses as well as from the BFKL inspired Monte Carlo BFKLex [28–32] is underway.

4 Conclusions

We performed a study of perturbative QCD in the high-energy limit through two different classes of processes. First we investigated the behaviour of cross section and azimuthal ratios for di-hadron production, which represents a less inclusive final state process with respect to the well known Mueller–Navelet jet

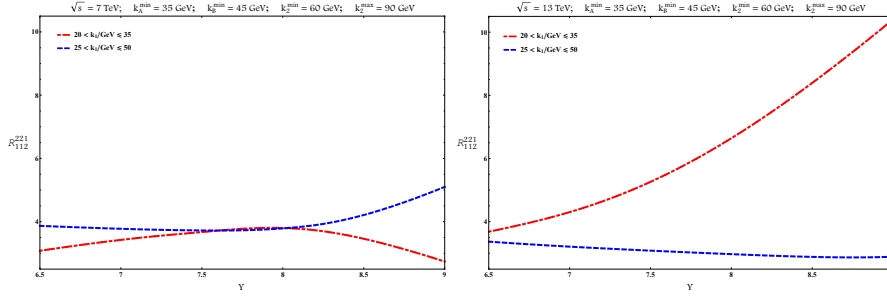


Figure 3: Y dependence of R_{112}^{221} for $\sqrt{s} = 7$ TeV (left column) and for $\sqrt{s} = 13$ TeV (right column). The rapidity interval between a jet and the closest one is fixed to $Y/3$.

reaction. Then we proposed to study multi-jet production processes, in order to define new, generalized and suitable BFKL observables. The comparison with experimental data will help to gauge and disentangle the applicability region of the BFKL formalism, therefore it is needed and suggested.

References

1. L.N. Lipatov, Sov. Phys. JETP **63** (1986) 904 [Zh. Eksp. Teor. Fiz. **90** (1986) 1536].
2. I.I. Balitsky and L.N. Lipatov, Sov. J. Nucl. Phys. **28** (1978) 822 [Yad. Fiz. **28** (1978) 1597].
3. E.A. Kuraev, L.N. Lipatov and V.S. Fadin, Sov. Phys. JETP **45** (1977) 199 [Zh. Eksp. Teor. Fiz. **72** (1977) 377].
4. E.A. Kuraev, L.N. Lipatov and V.S. Fadin, Sov. Phys. JETP **44** (1976) 443 [Zh. Eksp. Teor. Fiz. **71** (1976) 840] [Erratum-ibid. **45** (1977) 199].
5. L.N. Lipatov, Sov. J. Nucl. Phys. **23** (1976) 338 [Yad. Fiz. **23** (1976) 642].
6. V.S. Fadin, E.A. Kuraev and L.N. Lipatov, Phys. Lett. B **60** (1975) 50.
7. V.S. Fadin and L.N. Lipatov, Phys. Lett. B **429** (1998) 127 [hep-ph/9802290].
8. M. Ciafaloni and G. Camici, Phys. Lett. B **430** (1998) 349 [hep-ph/9803389].
9. A.H. Mueller and H. Navelet, Nucl. Phys. B **282** (1987) 727.
10. A. Sabio Vera, Nucl. Phys. B **746** (2006) 1 [hep-ph/0602250].
11. A. Sabio Vera and F. Schwennsen, Nucl. Phys. B **776** (2007) 170 [hep-ph/0702158 [HEP-PH]].

12. D. Colferai, F. Schwennsen, L. Szymanowski, S. Wallon, JHEP **1012** (2010) 026 [arXiv:1002.1365 [hep-ph]].
13. B. Ducloué, L. Szymanowski, S. Wallon, JHEP **1305** (2013) 096 [arXiv:1302.7012 [hep-ph]].
14. B. Ducloué, L. Szymanowski, S. Wallon, Phys. Rev. Lett. **112** (2014) 082003 [arXiv:1309.3229 [hep-ph]].
15. B. Ducloué, L. Szymanowski, S. Wallon, Phys. Lett. B **738** (2014) 311 [arXiv:1407.6593 [hep-ph]].
16. F. Caporale, D.Yu. Ivanov, B. Murdaca and A. Papa, Eur. Phys. J. C **74** (2014) 3084 [arXiv:1407.8431 [hep-ph]].
17. F.G. Celiberto, D.Yu. Ivanov, B. Murdaca and A. Papa, Eur. Phys. J. C **75** (2015) no.6, 292 [arXiv:1504.08233 [hep-ph]].
18. F.G. Celiberto, D.Yu. Ivanov, B. Murdaca and A. Papa, Eur. Phys. J. C **76** (2016) no.4, 224 [arXiv:1601.07847 [hep-ph]].
19. R. Ciesielski, arXiv:1409.5473 [hep-ex].
20. M. Angioni, G. Chachamis, J.D. Madrigal and A. Sabio Vera, Phys. Rev. Lett. **107**, 191601 (2011) [arXiv:1106.6172 [hep-th]].
21. G. Chachamis, arXiv:1512.04430 [hep-ph].
22. D.Yu. Ivanov and A. Papa, JHEP **1207** (2012) 045 [arXiv:1205.6068 [hep-ph]].
23. F.G. Celiberto, D.Yu. Ivanov, B. Murdaca and A. Papa, arXiv:1604.08013 [hep-ph].
24. F. Caporale, G. Chachamis, B. Murdaca and A. Sabio Vera, Phys. Rev. Lett. **116** (2016) no.1, 012001 [arXiv:1508.07711 [hep-ph]].
25. F. Caporale, F.G. Celiberto, G. Chachamis and A. Sabio Vera, Eur. Phys. J. C **76** (2016) no.3, 165 [arXiv:1512.03364 [hep-ph]].
26. F. Caporale, F.G. Celiberto, G. Chachamis, D.G. Gómez and A. Sabio Vera, arXiv:1603.07785 [hep-ph].
27. F. Caporale, F.G. Celiberto, G. Chachamis, D.G. Gómez and A. Sabio Vera, arXiv:1606.00574 [hep-ph].
28. G. Chachamis, M. Deak, A. Sabio Vera and P. Stephens, Nucl. Phys. B **849** (2011) 28 [arXiv:1102.1890 [hep-ph]].
29. G. Chachamis and A. Sabio Vera, Phys. Lett. B **709** (2012) 301 [arXiv:1112.4162 [hep-th]].
30. G. Chachamis and A. Sabio Vera, Phys. Lett. B **717** (2012) 458 [arXiv:1206.3140 [hep-th]].
31. G. Chachamis, A. Sabio Vera and C. Salas, Phys. Rev. D **87** (2013) 1, 016007 [arXiv:1211.6332 [hep-ph]].
32. G. Chachamis and A. Sabio Vera, JHEP **1602** (2016) 064 doi:10.1007/JHEP02(2016)064 [arXiv:1512.03603 [hep-ph]].